Effects of the sesquiterpene lactone parthenolide on prostate tumor-initiating cells: an integrated molecular profiling approach

Brian T. Kawasaki[1,*], **Elaine M. Hurt**[1,*], **Madhuri Kalathur**[1], **Maria Ana Duhagon**[1,2], **John A. Milner**[3], **Young S. Kim**[3], and **William L. Farrar**[1]

[1]*Cancer Stem Cell Section, Laboratory of Cancer Prevention, Center for Cancer Research, National Cancer Institute at Frederick (NCI-Frederick), National Institutes of Health, Frederick, MD 21702, USA.*

[2]*LIM- F. Ciencias, Igua 4225, CP 11400 / Genetica- F. Medicina, Gral. Flores 2125, CP 11800. Universidad de la República, Montevideo, Uruguay.*

[3]*Nutritional Science Research Group, Division of Cancer Prevention, National Cancer Institute, National Institutes of Health, Bethesda, MD 20892, USA.*

Abstract

Recent evidence suggests tumor-initating cells (TICs), also called cancer stem cells, are responsible for tumor initiation and progression; therefore, they represent an important cell population for development of future anti-cancer therapies. In this study, we show that the sesquiterpene lactone parthenolide (PTL) is cytotoxic to prostate TICs isolated from prostate cancer cell lines: DU145, PC3, VCAP and LAPC4, as well as primary prostate TICs. Furthermore, PTL inhibited TIC-driven tumor formation in mouse xenografts. Using an integrated molecular profiling approach encompassing proteomics, profiles of activated transcription factors and genomics we ascertained the effects of PTL on prostate cancer cells. In addition to the previously described effects of PTL, we determined that the non-receptor tyrosine kinase src, and many src signaling components, including: Csk, FAK, β1-arrestin, FGFR2, PKC, MEK/MAPK, CaMK, ELK-1 and ELK-1-dependent genes are novel targets of PTL action. Furthermore, PTL altered the binding of transcription factors important in prostate cancer including: C/EBP-α, fos related antigen-1 (FRA-1), HOXA-4, c-MYB, SNAIL, SP1, serum response factor (SRF), STAT3, X-box binding protein-1 (XBP1) and p53. In summary, we show PTL is cytotoxic to prostate TICs and describe the molecular events of PTL-mediated cytotoxicity. Therefore, PTL represents a promising therapeutic for prostate cancer treatment.

Keywords

prostate; cancer stem cells; parthenolide; phytonutrient

INTRODUCTION

For American men, prostate cancer has the highest incidence of all cancers and is the third leading cause of death behind heart disease and lung cancer. Treatment of prostate cancer involves radiotherapy, surgery, hormone therapy and chemotherapy depending on the stage of the disease [1]. Individuals with metastatic prostate cancer inevitably become refractory to

Corresponding Author: Dr. William L Farrar, NCI-Frederick, 1050 Boyles Street, Building 560, Room 21-78, Frederick, MD 21702, USA. E-mail: E-mail: farrar@mail.ncifcrf.gov.
*contributed equally to the work of this paper

conventional therapy, resulting in disease progression and death [2]. It is imperative that new treatments be developed to battle this fatal disease.

A growing body of evidence suggests a subpopulation of tumor-initiating cells (TICs) are the mediators of tumor initiation, progression and relapse [3]. These cells have the ability to self-renew, are multipotent and have a high proliferative capacity. These three qualities allow a TIC to generate the heterogeneous population of cells found within a tumor, while continually maintaining the regenerative pool of TICs. In contrast, the non-TICs, which are the majority of the tumor cells, have limited self-renewal capacity, are at the end stages of cellular differentiation and have minimal proliferative potential [4].

In prostate cancer, the CD44$^+$ cells are enriched for TICs [5,6]. Patrawala et al. showed that CD44$^+$ cells purified from a number of prostate cancer cell lines were more proliferative, clonogenic, tumorigenic, and metastatic than the corresponding CD44$^-$ cells [7]. In addition, tumors derived from xenografts of mice injected with CD44$^+$ cells histologically resembled tumors originating from unsorted cells. Furthermore, as few as 100 CD44$^+$ cells were able to form tumors whereas it required approximately 10-fold more CD44$^-$ cells to form a tumor. The CD44$^+$ cells purified from tumors expressed high levels of stem cell-associated genes, including *Oct-3/4, Bmi-1, β-catenin, and smoothened* [8], which is a characteristic of TICs.

The existence of prostate TICs has several important implications. First, it provides an explanation for how a heterogeneous tumor can be formed. The TICs are the founder population that gives rise to the various other non-tumorigenic cell types in the tumor. Second, TICs appear to be more resistant to conventional chemotherapy thereby leading to resistant disease [9]. Given these considerations, it is important that future treatments are effective against this cell population.

Epidemiological studies strongly suggest a diet rich in fruits and vegetables is associated with a lower risk in many cancers including prostate cancer [10]. Contained within many of these foods are phytochemicals, the active constituents in plants, that possess a number of chemopreventative characteristics, including: anti-neoplastic, anti-viral, anti-neurodegenerative, analgesic and anti-inflammatory properties [11]. These compounds represent a promising avenue in the treatment of cancer, as well as a non-toxic approach to chemoprevention. In addition, many chemopreventative agents can be used in combination with chemotherapeutic drugs at lowered doses in order to reduce adverse side effects [12].

The naturally occurring phytochemical, parthenolide (PTL), is a sesquiterpene lactone that occurs in the plant feverfew, a common medicinal herb traditionally used for headaches and arthritis. Recent evidence suggests PTL may be a useful therapeutic agent against certain cancers including: leukemias, breast and pancreatic carcinomas [13,14]. PTL has been shown to inhibit nuclear factor kappa-B (NF-κB) activation by binding and inhibiting IκB-kinase (IKK), an activator of NF-κB [15]. In addition, PTL inhibits both signal transducers and activators of transcription 3 (STAT3) after activation by interleukin-6 (IL-6), and c-jun N-terminal kinase (JNK) after activation by tumor necrosis factor-α (TNF-α) [16].

Recent studies suggest PTL may be effective in targeting cancer stem cells in some cancers. Guzman et al. showed PTL specifically targeted cancer stem cells in primary human acute myelogenous leukemia cells and blast crisis chronic myelogenous leukemia [17]. The mechanism of action was through inhibition of NFκB, activation of proapoptotic p53 and an increase in reactive oxygen species (ROS). Another study looked at PTL toxicity on two types of breast cancer TICs: the side population and the breast mammosphere [18]. Zhou et al. showed PTL was able to inhibit growth and colony formation of each of the tumor-initiating populations. In addition, NF-κB activity was reduced.

Given breast TICs are sensitive to PTL, we set out to investigate its role on targeting prostate cancer CD44^{+} TICs both *in vitro* and *in vivo*. Our study demonstrates PTL was cytotoxic to these cells isolated from prostate cancer cell lines and patients. Additionally, mouse xenograft studies showed PTL inhibited tumor initiation and progression by CD44^{+} TICs. We also determined the molecular mechanisms underlying PTL-induced toxicity in prostate cancer. Previous work on PTL offered a narrow view of the molecular mechanisms by which this compound acts. An integrated molecular profiling approach was used to examine early protein phosphorylation/expression events, transcription factor (TF) activation and gene expression patterns [19]. We found one of the early events of PTL cytotoxicity was attenuation of activity of the non-receptor tyrosine kinase, src and many src-associated signaling components that include: Csk, FAK, β1-arrestin, FGFR2, PI3K, PKC, MEK/MAPK, CaMK, the transcription factor ELK-1 and ELK-1 dependent genes. Additionally, we found PTL altered binding of a number of TFs involved in prostate cancer, including: C/EBP-α, FRA-1, HOXA-4, c-MYB, SNAIL, SP1, SRF, STAT1/3, XBP1 and p53. This is the first investigation to determine that prostate CD44^{+} TICs are sensitive to PTL targets and to study the effects of PTL on prostate cancer using an integrated molecular profiling approach. Given the estimated 28,660 men that will die of prostate cancer this year, new therapies are needed and PTL represents an encouraging therapeutic again for prostate cancer prevention and treatment.

MATERIALS AND METHODS

Cell Culture

Prostate cancer cell lines, DU145 and VCaP (ATCC, Manassas VA) were cultured in DMEM, PC3 (ATCC) in F-12 Kaighn's, LAPC4 (kind gift from Charles Sawyers, Memorial Sloan Kettering Cancer Center) in Iscove's DMEM. All cell lines were supplemented with 10% heat-inactivated FBS, 1% penicillin/streptomycin and 2mM L-glutamine and cultured in a 37°C, 5% CO_2 incubator. Sorted cells were cultured in a serum free medium as previously described [20]. Primary prostate cancer stem cells were purchased from Celprogen (San Pedro, CA) and maintained in Celprogen's Human Prostate Cancer Stem Cell Complete Growth Un-differentiating Medium.

Fluorescent Activated Cell Sorting (FACS)

Cells were detached with trypsin and washed once in FACS buffer (PBS containing 1–2% BSA and 5 mM EDTA). Washed cells were incubated at 4°C for 15 min with 5 µl/10^6 cells of anti-CD44 conjugated PE (Invitrogen, Carlsbad, CA). Cells were then washed in FACS buffer, re-suspended at 20 million cells/ml, and separated on a MoFlo High Performance cell sorter (Dako Cytomation, Carpinteria, CA).

Animal Studies

Mice were from NCI's Animal Genetics and Production Facility and housed in a pathogen free environment. NCI-Frederick is accredited by AAALAC International and follows the Public Health Service Policy for the Care and Use of Laboratory Animals. Animal care was provided in accordance with the procedures outlined in the "Guide for Care and Use of Laboratory Animals" (National Research Council; 1996; National Academy Press; Washington, D.C.). Injections were supplemented with an equal volume of Matrigel (BD Biosciences, Franklin Lakes, NJ) and animals were monitored weekly for palpable tumor formation. Stock solution of PTL (LKT Laboratories, St. Paul, MN) were prepared by first dissolving the powder in 100% ethanol and then diluting in saline (0.9% NaCl) to a 1:10, ethanol: saline ratio. The resultant slurry solution (100 µl) was administered by oral gavage and given at a dose of 10 mg/kg or 40 mg/kg, once daily, 3 times a week. Vehicle was a 1:10, ethanol: saline (0.9% NaCl) mixture.

Cell Viability Assay

Cells were plated at a density of 500 cells per well in a 96-well plate and viability was measured using Promega's Cell-Titer Glo assay (Madison, WI). The Cell-Titer Glo reagent was added to each well and equilibrated for 30 min before measurement was taken. Luminescence was measured using a M100 Tecan Luminometer (Research Triangle Park, NC).

Protein Microarray

Protein arrays were done using the Kinex™ antibody microarray service (Kinexus, Vancouver, BC, Canada). Cells were plated on a 150 mm dish (6×10^6 cells/dish) and PTL (10 µM) was added to each dish for 15 or 60 min. DMSO (0.1%) was used as the negative control. After PTL treatment, cells were rinsed twice with phosphate-buffered saline (PBS) and scraped off the plate. The cells were pelleted and lysed by adding 0.1 ml Kinexus lysis buffer (for details, see www.kinexus.ca). Cells were sonicated twice for 5 sec and the homogenate was subjected to centrifugation for 10 min at 14, 000 rpm. The protein concentration of the supernatant fraction was measured using the bicinchoninic acid protein assays (Pierce, Rockford, IL).

RNA Isolation

Total RNA was isolated using Invitrogen's Trizol reagent as per the manufacturer's instruction. Quantitation of RNA was carried out using a Nano-Drop ND100 Spectrophotometer (Wilmington, DE).

Transcription Array

Panomics DNA/protein combo arrays containing 345 consensus-binding sites were hybridized according to the manufacturer's instructions (Panomics, Fremont, CA). Nuclear protein was extracted from PTL-treated DU145 cells using Panomics' Nuclear Protein extraction kit following the manufacturer's instructions. Nuclear protein lysates (15 µg of each) were used in the binding reaction. Following cleanup, the probe was hybridized at 42°C overnight. Data were quantified using ImageQuant TL (Amersham Biosciences, Arlington Heights, IL).

Gene Expression Microarray

Gene expression microarrays were performed using Agilent Technology's (Santa Clara, CA) Whole Genome Expression Microarrays. After PTL treatment, the plates were washed twice in cold PBS and cells were harvested for RNA extraction. Ten µg of total RNA, from treated cells or universal RNA (Stratagene, La Jolla, CA), was labeled in a reverse transcriptase (RT) reaction mix as previously described [21]. Following labeling, RNAse H was added to each reaction for 30 min at RT. The Cy3 labeled reaction was mixed with Cy5-labeled reaction, and purified using an YM-30 Microcon column (Millipore, Billerica, MA) to an approximate volume of 44 µl. Purified probes were mixed with Agilent blocking buffer (11 µl) and hybridization buffer (55 µl). Agilent microarrays were hybridized to the mixture of Cy3 and Cy5-labeled probes, overnight, at 65°C. Slides were scanned in a GenePix 4000B scanner and analyzed using GenePix Pro (Molecular Devices, Sunnyvale, CA). Data analysis was performed using Cluster and TreeView offered by Michael B. Eisen (http://rana.lbl.gov/EisenSoftware.htm).

In-Cell Western (ICW)

Src expression (phosphorylation at Y529 and pan-specific) was performed using Li-Cor's infrared-based In-cell western assay. Sorted CD44+ DU145 cells were seeded in a 96-well plate (5,000 cells/well) and PTL (10 µM) was added to each well for 15, 30 or 60 min. DMSO (0.1%) was used as the negative control or "0" time point. After PTL treatment, cells were fixed and permeablized with methanol for 15 min, on ice. The cells were then blocked (PBS containing

2% fish gelatin), incubated with either a phosphospecific src antibody to tyrosine 529 (1:100 dilution; Cell Signaling, Danvers, MA) or a pan-specific src antibody (1:100; Abcam, Cambridge, MA), overnight at 4°C. The primary antibody was detected using an IRDye 800 infrared dye conjugated to a goat anti-rabbit secondary antibody (1:200 dilution; Li-Cor, Lincoln, NB). Antibody staining intensity was measured using Li-Cor's Odyssey Infrared Imaging System software. Quantitation was normalized to TO-PRO-3 iodide (1:4000), a nuclear stain.

RESULTS

Tumor-initiating cells are enriched for CD44 expression

Previous studies showed that prostate cancer cells expressing CD44 are enriched in tumorigenic and metastatic progenitors [22,23]. To validate this observation, we FACS sorted the top (CD44^{hi}) and bottom (CD44$^{-/lo}$) 5% of CD44 stained DU145 cells (Figure 1A) and subcutaneously injected them into NOD/SCID mice. After 3 months, tumors formed in 100% (6/6) of mice injected with CD44^{hi} cells whereas tumors formed in only 33% (2/6) of mice injected with CD44$^{-/lo}$ cells (Figure 1B). In addition, we previously determined that the CD44^{hi} cells formed colonies in an anchorage-independent manner at an approximately 2-fold higher rate than their CD44$^{-/lo}$ counterparts [24]. Hence, the CD44^{hi} population is enriched in TICs and we determined the effects of PTL toxicity on this important subpopulation.

Tumor-initiating prostate cancer stem cells are sensitive to parthenolide

Given that parthenolide is toxic to some cancer cells, we tested the effect of PTL (0–10 µM) on prostate cancer cell lines. PTL reduced viability of unsorted cells in a dose dependent manner over 72 hours (Figure 2A). When the four cell lines, DU145, PC3, VCAP and LAPC4, were treated with 5 µM PTL, we saw viability decrease to 12–28% as compared to vehicle treated cells. Increasing the concentration of PTL to 10 µM further reduced viability to 2–16% (LAPC4 and VCAP, respectively). To determine if PTL was effective against prostate cancer CD44^{+} TICs, we performed *in vitro* viability assays on both CD44^{hi} and CD44$^{-/lo}$ cells purified from several prostate cancer cell lines. As seen in Figure 2B and 2C, PTL was equally cytotoxic to both CD44$^{-/lo}$ and CD44^{hi} cells, respectively. After evaluating PTL efficacy on immortalized cell lines, we then addressed whether PTL was cytotoxic toTICs derived from patient samples.

We tested PTL toxicity on three primary prostate TICs (Figure 2D) obtained from Celprogen (San Pedro, CA). These cells were clonally selected from prostate cancer tissue originating from clinical specimens. The cells tested positive for the stem genes: *Oct-4, stage-specific embryonic antigen (SSEA)-3/4, alkaline phosphatase (AP) and prostate specific antigen (PSA)* (Celprogen, San Pedro, CA). Additionally, these cells were positive for: *CD44, Notch-1, SHH, Nanog and Bmi-1* and were highly tumorigenic (MAD unpublished results). Figure 2D shows the primary prostate TICs had decreased viability to PTL treatment similar to the four cancer cell lines (Figure 2A–C). Viability was decreased to 8–22% at 72 hr when treated with 10 µM PTL. Therefore, primary prostate TICs are also sensitive to PTL.

To further analyze PTL's efficacy, we determined if PTL could inhibit tumor-initiation *in vivo*. Using a NOD/SCID xenograft model, 100 CD44^{hi} DU145 cells, the previously identified TICs, were injected subcutaneously and split into the following groups; vehicle treated, or treated with PTL 3 times per week over the course of the entire experiment (up to 106 days) at two concentrations (10 mg/kg and 40 mg/kg). As shown in Figure 3, PTL reduced both tumor incidence and tumor latency. At 85 days, 100% of vehicle treated mice had tumors, whereas only 67% (4/6) of 10 mg/kg PTL treated mice had tumors and 50% (3/6) of 40 mg/kg PTL treated mice had tumors. The average latency period for vehicle treated was 61 days, whereas the average latency period was 74 and 77.5 days for 10 mg/kg and 40 mg/kg, respectively.

Taken together, this data shows PTL was able to reduce tumor incidence and latency initiated by TICs in a dose-dependent manner. We next turned our attention to elucidating the molecular mechanisms of PTL toxicity using an integrated molecular profiling approach.

Protein microarray analysis of PTL action

Given our data indicating PTL killed all of the cell lines (DU145, PC3, VCAP and LAPC4) and populations (CD44^{hi}, CD44^{−/lo} and unsorted) with similar dose-responses (Figure 2A–C), we inferred the molecular events of PTL-mediated cytotoxicity were also similar. Therefore, we carried out our profiling approach on the unsorted DU145 population. Our first goal was to identify early protein phosphorylation events and protein expression changes. We used Kinexus antibody microarrays that interrogate 273 phospho-specific proteins and 377 pan-specific proteins. DU145 cells were treated with 10 µM PTL for 15 or 60 min. From 650 proteins, we found 194 proteins that changed 2-fold or greater (phosphorylation or expression) at 15 or 60 min or both time points (Supplemental Figure 1). Interestingly, we found the non-receptor tyrosine kinase src and many src-related signaling components were affected by PTL treatment (Figure 4A). Src is involved in androgen receptor transactivation, tumor proliferation and invasion in prostate cancer [25]. We observed an increase in phosphorylation of src at tyrosine-529, which indicates a decrease in src activity [26].

Additionally, there were four proteins known to be direct regulators of src activity [26] that were affected by PTL treatment: Csk, FAK, β1-arrestin and FGFR2 (Figure 4A, top left panel). Csk, the kinase that phosphorylates src at Y529 [26], showed an increase in expression in response to PTL. We detected a decrease in expression/phosphorylation of β1-arrestin, FAK and FGFR2, all known activators of src. Downstream signaling proteins of src that were also affected by PTL include PI3K, PKCs, MAPK/MEKs, and CaMKs (Figure 4A). Nine out of 13 PKCs, 8 out of 13 MEK/MAPKs, and 3 out of 4 CaMKs showed a loss of protein expression or phosphorylation. Other proteins also found to be modulated by PTL were c-JUN, JNK and STAT3 (Supplemental Figure 1) where previous work has shown that these proteins are affected by PTL treatment [27].

Parthenolide induces alterations in transcription factor binding

Our next goal was to look at early transcription factor binding events induced by PTL treatment. To achieve this, we used Panomic's Protein/DNA array that measures DNA binding of 345 transcription factors. DU145 cells were treated with 10 µM PTL for 30 or 90 min, or DMSO (0.1%) as a control. There were 39 TFs with decreased and 18 with increased DNA-binding activity (Supplemental Table 1). We assigned "fold-changes in binding" to sites with visible spots on the array (Figure 4B). Any potential decrease in binding where there was no visible spot was labeled "undetectable." To further evaluate our data, we looked for TF binding changes that were relevant to prostate cancer and found the following: C/EBP-α, fos-related antigen (FRA-1), ELK-1, homeobox A4 (HOXA-4), c-MYB, p53, SNAIL, SP1, serum response factor (SRF), STAT1/3 and X-box binding protein-1 (XBP1)(Supplemental Table 1). Each of these TFs are linked to prostate cancer initiation, progression or metastasis [28–34]. For example, HOXA-4 is a potential clinical marker for prostate cancer [35] and STAT3 activation is associated with tumor metastasis in prostate cancer [36]. Interestingly, ELK-1, a downstream target of src, showed a significant decrease in binding at both time points (Figure 4B). ELK-1 stimulates cell proliferation and sustains tumor growth in prostate cancer [37]. Therefore, we demonstrate that all components of the src/MAPK/ELK-1 signaling pathway are downregulated by PTL treatment (Figure 4A–C).

Gene Expression Changes Induced by Parthenolide

To complete our integrated profiling approach, we analyzed gene expression changes induced by PTL, using Agilent's Human Whole Genome Expression Microarrays. Either PTL (10 µM)

or DMSO (0.1%) was added to DU145 cells for 1, 4 or 8 hr. Our analysis found 387 genes, 118 upregulated and 269 downregulated, that changed at least 2-fold in any time point (Supplemental Figure 2a–e).

To further analyze our PTL gene set (387 total genes), we identified TF binding sites in the PTL-regulated genes using the Gene Set Enrichment Analysis (GSEA, http://www.broad.mit.edu/gsea/, Broad Institute, Cambridge, MA) that analyzes 500 TF binding sites. Our analysis found 36 TF binding sites in the PTL-regulated genes (Supplemental Table 2). To refine our analysis, we next determined if any of the 36 TFs were involved in prostate cancer and, we indeed found 17 TFs that have been implicated or directly involved in prostate malignancy: the androgen receptor, CDX2, C/EBP-α, C/EBP-β, EGR1, ELK-1, ETS1, ETS2, FOXA1, GFI1, JUN, LEF1, c-MYB, c-MYC, SMAD3 and SP1 [28, 38–44]. The TFs overlapping with those we found using Panomic's protein/DNA array (Supplemental Table 1) include: C/EBP-α, JUN, c-MYB, SP1 and ELK-1. Interestingly, we found 15 ELK-1-associated genes were modulated by PTL, with 10 out of 15 having a decrease in expression (Figure 4C), consistent with and further validating the decrease in binding we found on the TF array (Figure 4B).

Given that we saw similar levels of PTL toxicity in both the total cell population and in the CD44^{+} TICs and that src activation was indentified as a mediator of PTL-induced cytotoxicity in the total cell population, we wished to validate the inactivation of src in DU145 TICs. Therefore, we evaluated attenuation of src activity in the CD44^{hi} TICs using Li-Cor's In-cell western assay (Figure 5A and B). Sorted CD44^{hi} DU145 cells were treated with PTL (10 µM) for 15, 30 and 60 min and measured for src phosphorylation at tyrosine 529. As shown in Figure 5B, there was a 68, 56 and 48% increase in phosphorylation at 15, 30 and 60 min, respectively, indicating a decrease in src activity. Moreover, PTL treatment did not significantly affect the levels of total src expression. Finally, treatment of CD44^{hi} cells with PP2, a src inhibitor, showed a dose-dependent decrease in cellular viability as compared to the controls (Supplemental Figure 3). Taken together, our data suggests PTL-mediated cytotoxicity is mediated, in part, by attenuation of src signaling. Additionally, and more importantly, we validated the attenuation of src activity in TICs. Taken together, this indicates that one of the early signaling events of PTL treatment of prostate cancer cells is the downregulation of this signaling pathway in both the TICs as well as the non-TICs, indicating that PTL may be a viable treatment for prostate cancer.

DISCUSSION

This is the first study to demonstrate that the phytochemical parthenolide is able to induce cell death in prostate TICs. After 72 hrs of treatment with PTL (10 µM), we determined that it is toxic (>90%) to most of the TICs and non-TICs in both cell lines and primary prostate cancer cells (see Figure 2). The significance of these *in vitro* studies was validated using *in vivo* models. Mice engrafted with TICs and treated with PTL showed a marked decrease in tumor incidence and latency (see Figure 3). This suggests that PTL is a potential anti-prostate cancer agent that can target both the TICs and their differentiated progeny. In order to address the molecular targets of PTL, we performed an integrated molecular profiling of PTL cytotoxicity using protein microarrays (650 data points), transcription factor binding assays (345 data points) and genomic microarrays (whole genome). Collectively, we evaluated a high density of data points examining the status of numerous cellular functions. Our integrated molecular profiling approach was successful in following the effects of a drug's signal transduction process initiated at the plasma membrane down to regulation of TFs and finally to the corresponding gene expression level. In addition, we demonstrate each array set (protein, TF or gene expression) was able to validate one of the other array set (e.g. loss of ELK-1 binding in the TF array corresponded to loss of gene expression of many ELK-1 mediated genes in the

cDNA microarrays). Our results confirmed that previously reported proteins, such as STAT3 and JNK, are involved in PTL-induced cytotoxic effects (see Supplemental Figure 1)[45]. Interestingly, src activation was decreased upon addition of PTL (see Figure 4A), identifying this non-receptor tyrosine kinase as a novel target of PTL. We also saw attenuation of downstream src effectors, including: PI3K, PKCs, CaMKs and MAPKs (see Figure 4A). Finally, we confirmed one of the early events of our profiling, attenuation of src activity, in tumor-initiating cells using other biochemical methods (e.g. In-cell westerns). Future studies will validate the role of other signaling components of PTL cytotoxicity (e.g. MAPK, ELK-1) in the tumor-initiating population.

Src is a gateway signaling protein and is strongly implicated in prostate cancer [46]. It can promote crosstalk between numerous proteins that include G-protein coupled receptors, growth factor receptors (EGFR, PDGF and IGF), cytokine receptors and integrins, all of which have been implicated in cancers [47,48]. There are nine known family members in the src family of tyrosine kinases, but src itself is implicated most in cancer [49]. In particular, src has an important role in prostate cancer where it is overexpressed and src inhibitors attenuate cancer cell line growth and proliferation [50]. In addition, src has been implicated in bone metastasis of prostate cancer [51]. Given src's role in cell signaling and cancer, there are a number of src inhibitors already in various stages of clinical trials [52]. In particular, dasatinib, a novel src family tyrosine kinase and Abl kinase inhibitor is currently being evaluated for clinical trials in prostate cancer [53]. Given our studies showing PTL cytotoxicity attenuates src activity, future studies are warranted to evaluate the effectiveness of PTL in targeting prostate tumor cells.

An important hurdle in drug therapy development is overcoming solubility and bioavailability of the compound. Although, our *in vivo* studies showed PTL abrogated tumor initiation and latency, we found it was unable to do this proportionally to its dose (from 10 to 40 mg/kg). Contributing to this discrepancy is the solubility and bioavailability of PTL which was soluble at 10 mg/kg, but relatively insoluble at 40 mg/kg. Furthermore, previous work in animal models showed PTL reaches only nanomolar levels in serum [54]. At these concentrations, PTL would have to be increased almost 30 fold to reach cytotoxic *in vitro* levels [55]. Interestingly, a recent study discovered a PTL analog, dimethylaminoparthenolide (DMAPT) with 1000-fold increased solubility over PTL and a 70% oral bioavailability [56]. The drug had similar *in vitro* and *in vivo* cytotoxic affects and molecular responses as PTL. Moreover, DMAPT had *in vivo* activity in a canine leukemic model.

PTL's ability to target TICs is important to future therapies. These biologically unique cells are responsible for cancer initiation, progression, relapse and drug resistance [57]. The existence of TICs and their ability to self-renew, differentiate into multiple lineages and their unlimited proliferative capacity makes them particularly insidious to tumor malignancy. It is likely that the recurrence of a tumor results from the inability of the conventional therapy to target the cancer stem cell [58]. Therefore, it is paramount that future therapies target this vitally important population of cells. Our data shows that PTL treatment targets both prostate non-TICs as well as TICs, offering a novel therapy that may overcome the problem of tumor relapse and metastasis.

Here, we have uniquely identified the effects of PTL on src-initiated signaling pathways in prostate tumor-initiating cells. Additionally, PTL affects a number protein expression/ phosphorylation events, modulates transcription factors and gene expression. Specifically, PTL was shown to inhibit NFκB, STAT3 activities/proteins, suggesting that PTL may impact several pathways recognized to be involved in the etiology of prostate cancer (Figure 6). Importantly, our integrated molecular profiling has revealed that PTL may affect significant

pathways in prostate TICs, including the novel identification of the src pathway. Thus, PTL, or its analogs, may eventually be among the most efficacious treatment for patients.

Supplementary Material

Refer to Web version on PubMed Central for supplementary material.

Acknowledgments

Reference List

1. Sharifi N, Kawasaki BT, Hurt EM, Farrar WL. Stem cells in prostate cancer: resolving the castrate-resistant conundrum and implications for hormonal therapy. Cancer Biol Ther 2006;5:901–906. [PubMed: 16855379]

2. Sharifi N, Kawasaki BT, Hurt EM, Farrar WL. Stem cells in prostate cancer: resolving the castrate-resistant conundrum and implications for hormonal therapy. Cancer Biol Ther 2006;5:901–906. [PubMed: 16855379]

3. Dean M, Fojo T, Bates S. Tumour stem cells and drug resistance. Nat Rev Cancer 2005;5:275–284. [PubMed: 15803154]

4. Tang DG, Patrawala L, Calhoun T, Bhatia B, Choy G, Schneider-Broussard R, Jeter C. Prostate cancer stem/progenitor cells: identification, characterization, and implications. Mol Carcinog 2007;46:1–14. [PubMed: 16921491]

5. Patrawala L, Calhoun T, Schneider-Broussard R, Li H, Bhatia B, Tang S, Reilly JG, Chandra D, Zhou J, Claypool K, Coghlan L, Tang DG. Highly purified CD44+ prostate cancer cells from xenograft human tumors are enriched in tumorigenic and metastatic progenitor cells. Oncogene 2006;25:1696–1708. [PubMed: 16449977]

6. Hurt EM, Kawasaki BT, Klarmann GJ, Thomas SB, Farrar WL. CD44(+)CD24(−) prostate cells are early cancer progenitor/stem cells that provide a model for patients with poor prognosis. Br J Cancer 2008;98:756–765. [PubMed: 18268494]

7. Patrawala L, Calhoun T, Schneider-Broussard R, Li H, Bhatia B, Tang S, Reilly JG, Chandra D, Zhou J, Claypool K, Coghlan L, Tang DG. Highly purified CD44+ prostate cancer cells from xenograft human tumors are enriched in tumorigenic and metastatic progenitor cells. Oncogene 2006;25:1696–1708. [PubMed: 16449977]

8. Patrawala L, Calhoun T, Schneider-Broussard R, Li H, Bhatia B, Tang S, Reilly JG, Chandra D, Zhou J, Claypool K, Coghlan L, Tang DG. Highly purified CD44+ prostate cancer cells from xenograft human tumors are enriched in tumorigenic and metastatic progenitor cells. Oncogene 2006;25:1696–1708. [PubMed: 16449977]

9. Dean M, Fojo T, Bates S. Tumour stem cells and drug resistance. Nat Rev Cancer 2005;5:275–284. [PubMed: 15803154]

10. Aggarwal BB, Shishodia S. Molecular targets of dietary agents for prevention and therapy of cancer. Biochem Pharmacol 2006;71:1397–1421. [PubMed: 16563357]

11. Aggarwal BB, Shishodia S. Molecular targets of dietary agents for prevention and therapy of cancer. Biochem Pharmacol 2006;71:1397–1421. [PubMed: 16563357]

12. Aggarwal BB, Shishodia S. Molecular targets of dietary agents for prevention and therapy of cancer. Biochem Pharmacol 2006;71:1397–1421. [PubMed: 16563357]

13. Guzman ML, Rossi RM, Karnischky L, Li X, Peterson DR, Howard DS, Jordan CT. The sesquiterpene lactone parthenolide induces apoptosis of human acute myelogenous leukemia stem and progenitor cells. Blood 2005;105:4163–4169. [PubMed: 15687234]

14. Zhou, J.; Zhang, H.; Gu, P.; Bai, J.; Margolick, JB.; Zhang, Y. NF-kappaB pathway inhibitors preferentially inhibit breast cancer stem-like cells. Breast Cancer Res Treat. 2007.

15. Hehner SP, Hofmann TG, Droge W, Schmitz ML. The antiinflammatory sesquiterpene lactone parthenolide inhibits NF-kappa B by targeting the I kappa B kinase complex. J Immunol 1999;163:5617–5623. [PubMed: 10553091]

16. Guzman ML, Jordan CT. Feverfew: weeding out the root of leukaemia. Expert Opin Biol Ther 2005;5:1147–1152. [PubMed: 16120045]

17. Guzman ML, Rossi RM, Karnischky L, Li X, Peterson DR, Howard DS, Jordan CT. The sesquiterpene lactone parthenolide induces apoptosis of human acute myelogenous leukemia stem and progenitor cells. Blood 2005;105:4163–4169. [PubMed: 15687234]

18. Zhou, J.; Zhang, H.; Gu, P.; Bai, J.; Margolick, JB.; Zhang, Y. NF-kappaB pathway inhibitors preferentially inhibit breast cancer stem-like cells. Breast Cancer Res Treat. 2007.

19. Hurt EM, Thomas SB, Peng B, Farrar WL. Integrated molecular profiling of SOD2 expression in multiple myeloma. Blood 2007;109:3953–3962. [PubMed: 17192397]

20. Hurt EM, Kawasaki BT, Klarmann GJ, Thomas SB, Farrar WL. CD44(+)CD24(−) prostate cells are early cancer progenitor/stem cells that provide a model for patients with poor prognosis. Br J Cancer 2008;98:756–765. [PubMed: 18268494]

21. Hurt EM, Thomas SB, Peng B, Farrar WL. Integrated molecular profiling of SOD2 expression in multiple myeloma. Blood 2007;109:3953–3962. [PubMed: 17192397]

22. Patrawala L, Calhoun T, Schneider-Broussard R, Li H, Bhatia B, Tang S, Reilly JG, Chandra D, Zhou J, Claypool K, Coghlan L, Tang DG. Highly purified CD44+ prostate cancer cells from xenograft human tumors are enriched in tumorigenic and metastatic progenitor cells. Oncogene 2006;25:1696–1708. [PubMed: 16449977]

23. Hurt EM, Kawasaki BT, Klarmann GJ, Thomas SB, Farrar WL. CD44(+)CD24(−) prostate cells are early cancer progenitor/stem cells that provide a model for patients with poor prognosis. Br J Cancer 2008;98:756–765. [PubMed: 18268494]

24. Hurt EM, Kawasaki BT, Klarmann GJ, Thomas SB, Farrar WL. CD44(+)CD24(−) prostate cells are early cancer progenitor/stem cells that provide a model for patients with poor prognosis. Br J Cancer 2008;98:756–765. [PubMed: 18268494]

25. Asim, M.; Siddiqui, IA.; Hafeez, BB.; Baniahmad, A.; Mukhtar, H. Src kinase potentiates androgen receptor transactivation function and invasion of androgen-independent prostate cancer C4-2 cells. Oncogene. 2008.

26. Thomas SM, Brugge JS. Cellular functions regulated by Src family kinases. Annu Rev Cell Dev Biol 1997;13:513–609. [PubMed: 9442882]

27. Guzman ML, Jordan CT. Feverfew: weeding out the root of leukaemia. Expert Opin Biol Ther 2005;5:1147–1152. [PubMed: 16120045]

28. Yin H, Radomska HS, Tenen DG, Glass J. Down regulation of PSA by C/EBPalpha is associated with loss of AR expression and inhibition of PSA promoter activity in the LNCaP cell line. BMC Cancer 2006;6:158. [PubMed: 16774685]

29. Kaur M, Agarwal R. Transcription factors: molecular targets for prostate cancer intervention by phytochemicals. Curr Cancer Drug Targets 2007;7:355–367. [PubMed: 17979630]

30. de PG, Legrier ME, Poirson-Bichat F, Courty Y, Bras-Goncalves R, Dutrillaux AM, Nemati F, Oudard S, Lidereau R, Broqua P, Junien JL, Dutrillaux B, Poupon MF. Clinical and experimental progression of a new model of human prostate cancer and therapeutic approach. Am J Pathol 2001;159:753–764. [PubMed: 11485933]

31. Wang Q, Williamson M, Bott S, Brookman-Amissah N, Freeman A, Nariculam J, Hubank MJ, Ahmed A, Masters JR. Hypomethylation of WNT5A, CRIP1 and S100P in prostate cancer. Oncogene 2007;26:6560–6565. [PubMed: 17486081]

32. Beach, S.; Tang, H.; Park, S.; Dhillon, AS.; Keller, ET.; Kolch, W.; Yeung, KC. Snail is a repressor of RKIP transcription in metastatic prostate cancer cells. Oncogene. 2007.

33. Heemers HV, Regan KM, Dehm SM, Tindall DJ. Androgen induction of the androgen receptor coactivator four and a half LIM domain protein-2: evidence for a role for serum response factor in prostate cancer. Cancer Res 2007;67:10592–10599. [PubMed: 17975004]

34. Takahashi S, Suzuki S, Inaguma S, Ikeda Y, Cho YM, Nishiyama N, Fujita T, Inoue T, Hioki T, Sugimura Y, Ushijima T, Shirai T. Down-regulation of human Xbox binding protein 1 (hXBP-1) expression correlates with tumor progression in human prostate cancers. Prostate 2002;50:154–161. [PubMed: 11813207]

35. de PG, Legrier ME, Poirson-Bichat F, Courty Y, Bras-Goncalves R, Dutrillaux AM, Nemati F, Oudard S, Lidereau R, Broqua P, Junien JL, Dutrillaux B, Poupon MF. Clinical and experimental progression of a new model of human prostate cancer and therapeutic approach. Am J Pathol 2001;159:753–764. [PubMed: 11485933]

36. Horinaga M, Okita H, Nakashima J, Kanao K, Sakamoto M, Murai M. Clinical and pathologic significance of activation of signal transducer and activator of transcription 3 in prostate cancer. Urology 2005;66:671–675. [PubMed: 16140113]

37. Peterziel H, Mink S, Schonert A, Becker M, Klocker H, Cato AC. Rapid signalling by androgen receptor in prostate cancer cells. Oncogene 1999;18:6322–6329. [PubMed: 10597231]

38. Herawi M, De Marzo AM, Kristiansen G, Epstein JI. Expression of CDX2 in benign tissue and adenocarcinoma of the prostate. Hum Pathol 2007;38:72–78. [PubMed: 16949907]

39. Xiao W, Hodge DR, Wang L, Yang X, Zhang X, Farrar WL. Co-operative functions between nuclear factors NFkappaB and CCAT/enhancer-binding protein-beta (C/EBP-beta) regulate the IL-6 promoter in autocrine human prostate cancer cells. Prostate 2004;61:354–370. [PubMed: 15389813]

40. Mirosevich J, Gao N, Gupta A, Shappell SB, Jove R, Matusik RJ. Expression and role of Foxa proteins in prostate cancer. Prostate 2006;66:1013–1028. [PubMed: 16001449]

41. Dwivedi PP, Anderson PH, Omdahl JL, Grimes HL, Morris HA, May BK. Identification of growth factor independent-1 (GFI1) as a repressor of 25-hydroxyvitamin D 1-alpha hydroxylase (CYP27B1) gene expression in human prostate cancer cells. Endocr Relat Cancer 2005;12:351–365. [PubMed: 15947108]

42. Edlund S, Lee SY, Grimsby S, Zhang S, Aspenstrom P, Heldin CH, Landstrom M. Interaction between Smad7 and beta-catenin: importance for transforming growth factor beta-induced apoptosis. Mol Cell Biol 2005;25:1475–1488. [PubMed: 15684397]

43. Kaur M, Agarwal R. Transcription factors: molecular targets for prostate cancer intervention by phytochemicals. Curr Cancer Drug Targets 2007;7:355–367. [PubMed: 17979630]

44. Wang Q, Williamson M, Bott S, Brookman-Amissah N, Freeman A, Nariculam J, Hubank MJ, Ahmed A, Masters JR. Hypomethylation of WNT5A, CRIP1 and S100P in prostate cancer. Oncogene 2007;26:6560–6565. [PubMed: 17486081]

45. Guzman ML, Jordan CT. Feverfew: weeding out the root of leukaemia. Expert Opin Biol Ther 2005;5:1147–1152. [PubMed: 16120045]

46. Fizazi K. The role of Src in prostate cancer. Ann Oncol 2007;18:1765–1773. [PubMed: 17426060]

47. Hahn WC, Weinberg RA. Rules for making human tumor cells. N Engl J Med 2002;347:1593–1603. [PubMed: 12432047]

48. Bhola NE, Grandis JR. Crosstalk between G-protein-coupled receptors and epidermal growth factor receptor in cancer. Front Biosci 2008;13:1857–1865. [PubMed: 17981673]

49. Fizazi K. The role of Src in prostate cancer. Ann Oncol 2007;18:1765–1773. [PubMed: 17426060]

50. Chang YM, Kung HJ, Evans CP. Nonreceptor tyrosine kinases in prostate cancer. Neoplasia 2007;9:90–100. [PubMed: 17357254]

51. Myoui A, Nishimura R, Williams PJ, Hiraga T, Tamura D, Michigami T, Mundy GR, Yoneda T. C-SRC tyrosine kinase activity is associated with tumor colonization in bone and lung in an animal model of human breast cancer metastasis. Cancer Res 2003;63:5028–5033. [PubMed: 12941830]

52. Fizazi K. The role of Src in prostate cancer. Ann Oncol 2007;18:1765–1773. [PubMed: 17426060]

53. Fizazi K. The role of Src in prostate cancer. Ann Oncol 2007;18:1765–1773. [PubMed: 17426060]

54. Sweeney CJ, Mehrotra S, Sadaria MR, Kumar S, Shortle NH, Roman Y, Sheridan C, Campbell RA, Murry DJ, Badve S, Nakshatri H. The sesquiterpene lactone parthenolide in combination with docetaxel reduces metastasis and improves survival in a xenograft model of breast cancer. Mol Cancer Ther 2005;4:1004–1012. [PubMed: 15956258]

55. Guzman ML, Rossi RM, Neelakantan S, Li X, Corbett CA, Hassane DC, Becker MW, Bennett JM, Sullivan E, Lachowicz JL, Vaughan A, Sweeney CJ, Matthews W, Carroll M, Liesveld JL, Crooks PA, Jordan CT. An orally bioavailable parthenolide analog selectively eradicates acute myelogenous leukemia stem and progenitor cells. Blood 2007;110:4427–4435. [PubMed: 17804695]

56. Guzman ML, Rossi RM, Neelakantan S, Li X, Corbett CA, Hassane DC, Becker MW, Bennett JM, Sullivan E, Lachowicz JL, Vaughan A, Sweeney CJ, Matthews W, Carroll M, Liesveld JL, Crooks PA, Jordan CT. An orally bioavailable parthenolide analog selectively eradicates acute myelogenous leukemia stem and progenitor cells. Blood 2007;110:4427–4435. [PubMed: 17804695]

57. Dean M, Fojo T, Bates S. Tumour stem cells and drug resistance. Nat Rev Cancer 2005;5:275–284. [PubMed: 15803154]

58. Al-Hajj M, Becker MW, Wicha M, Weissman I, Clarke MF. Therapeutic implications of cancer stem cells. Curr Opin Genet Dev 2004;14:43–47. [PubMed: 15108804]

59. Subramanian A, Tamayo P, Mootha VK, Mukherjee S, Ebert BL, Gillette MA, Paulovich A, Pomeroy SL, Golub TR, Lander ES, Mesirov JP. Gene set enrichment analysis: a knowledge-based approach for interpreting genome-wide expression profiles. Proc Natl Acad Sci U S A 2005;102:15545–15550. [PubMed: 16199517]

60. Mootha VK, Lindgren CM, Eriksson KF, Subramanian A, Sihag S, Lehar J, Puigserver P, Carlsson E, Ridderstrale M, Laurila E, Houstis N, Daly MJ, Patterson N, Mesirov JP, Golub TR, Tamayo P, Spiegelman B, Lander ES, Hirschhorn JN, Altshuler D, Groop LC. PGC-1alpha-responsive genes involved in oxidative phosphorylation are coordinately downregulated in human diabetes. Nat Genet 2003;34:267–273. [PubMed: 12808457]
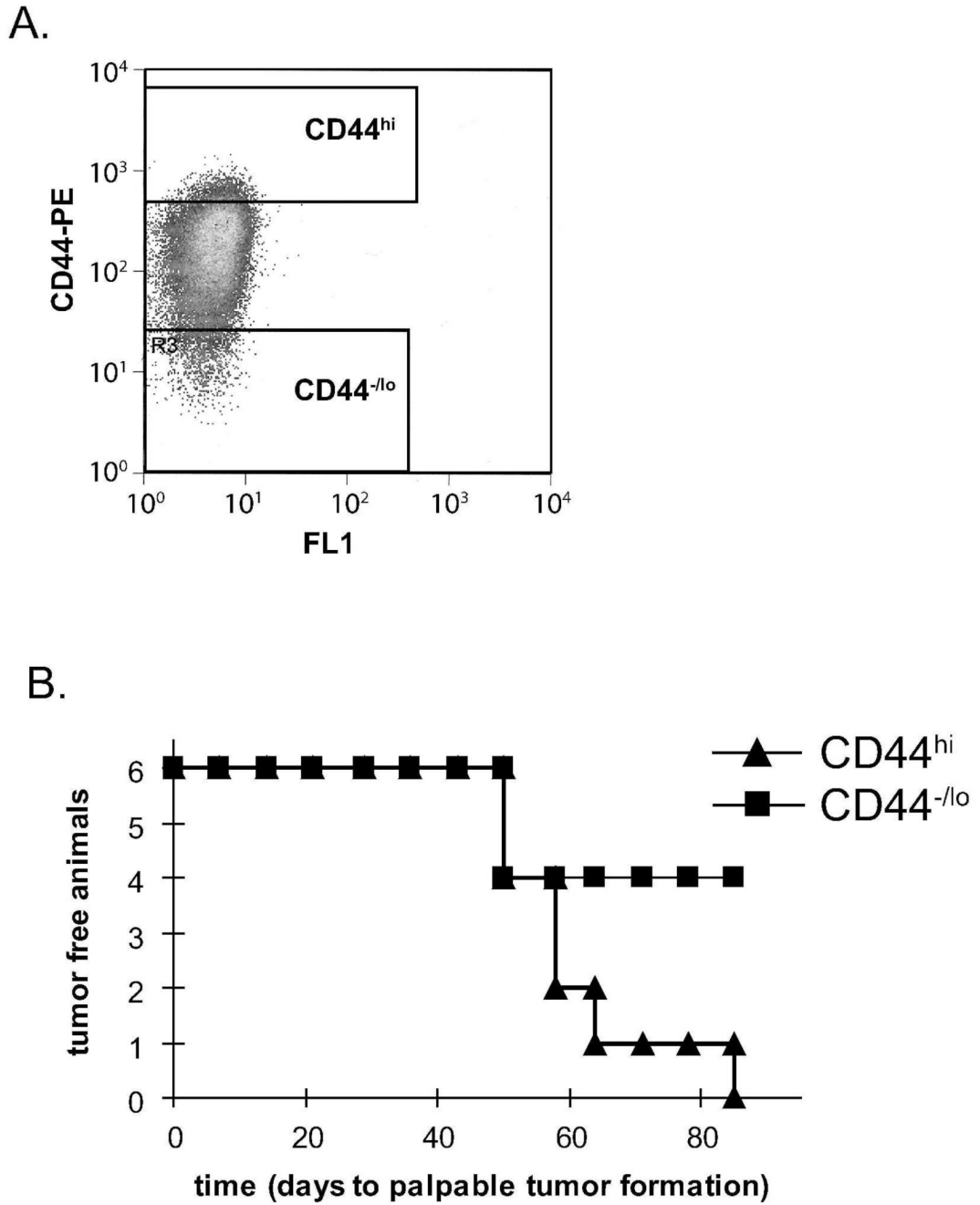
A.

B.

Figure 1.
CD44^{hi} is the cancer initiating population of cells. (A) DU145 cells were FACS sorted into two populations: the highest (CD44^{hi}) and lowest (CD44^{−/lo}) 5% of CD44 stained cells. (B) Kaplan-Meier plot for time to palpable tumor formation. CD44^{hi} and CD44^{−/lo} (100 sorted cells) were injected subcutaneously into the left and right flanks, respectively, of 6-week old NOD/SCID mice.
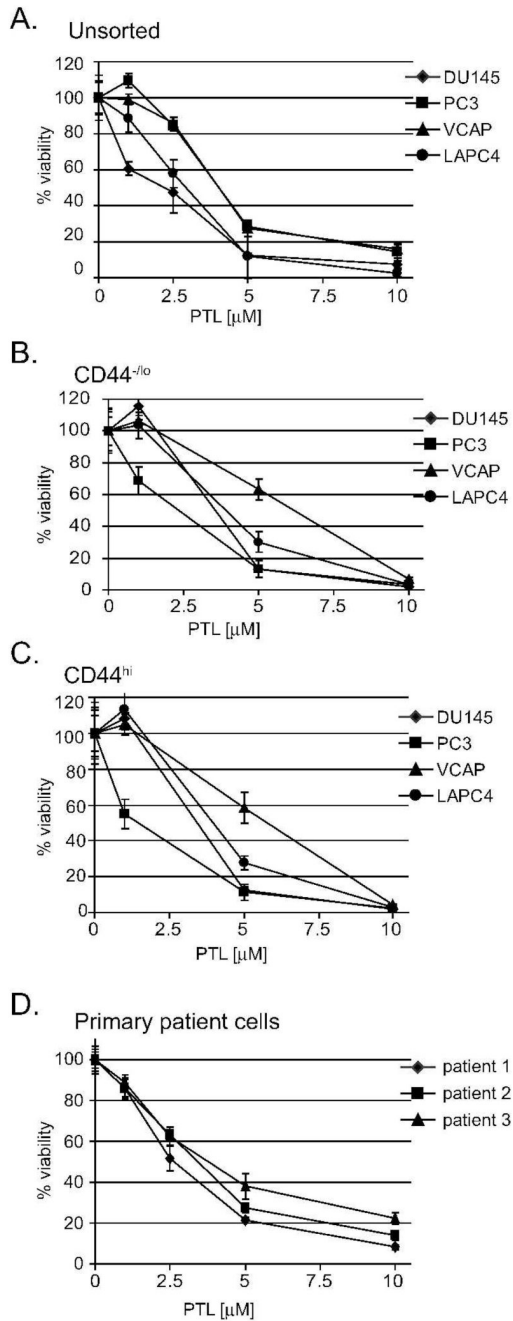
Figure 2.
Parthenolide targets both cancer stem and non-stem populations in prostate cancer cell lines and in cell lines derived from primary tissue. (A), unsorted (B) CD44^{−/lo} (C) CD44^{hi} and (D) primary tissue-derived cells were treated with various concentrations (0–10 µM) of PTL for 72 hr. Error bars represent standard deviations (SD). Y-axis represents percent viability normalized to untreated (0.1% DMSO) control. All experiments were done in triplicate and were performed at least three times, with representative experiment shown.
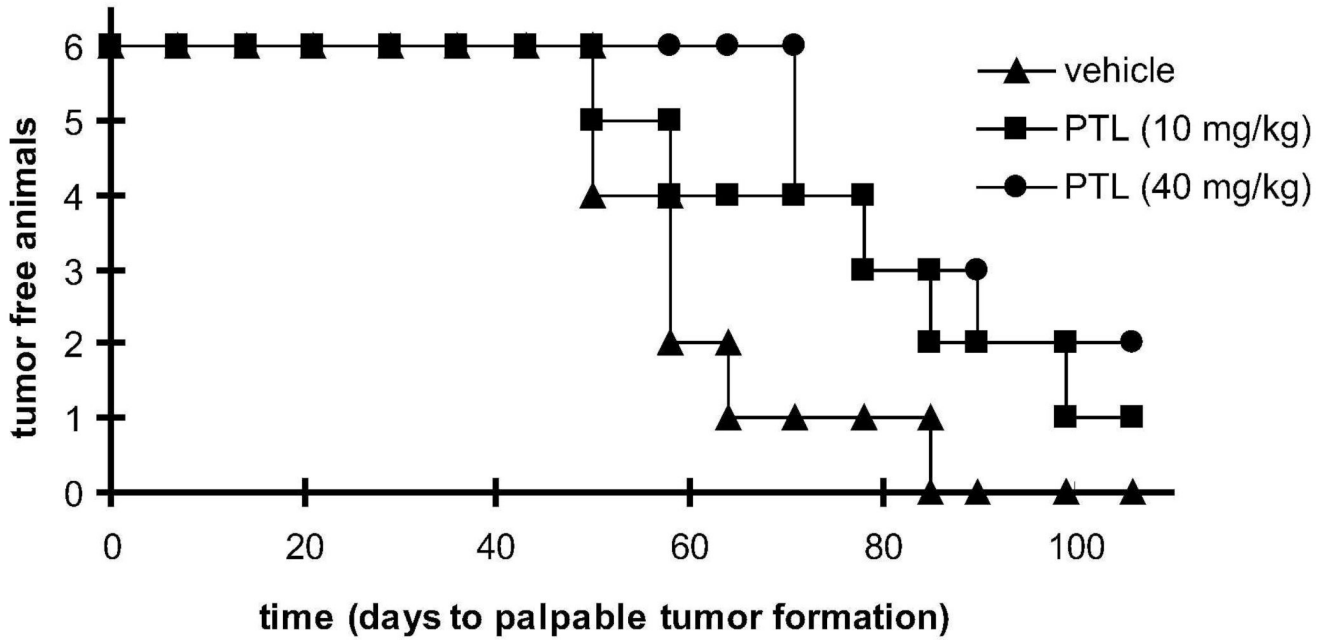
Figure 3.
Parthenolide targets prostate tumor-initiating cells *in vivo*. Figure shows a Kaplan-Meier plot of time to palpable tumor formation. CD44^{hi} (100 cells) were injected into the flank of male, 6-week old NOD/SCID mice and then split into the indicated treatment groups; closed triangle vehicle treated, closed square 10 mg/kg PTL, and closed circle 40 mg/kg PTL.
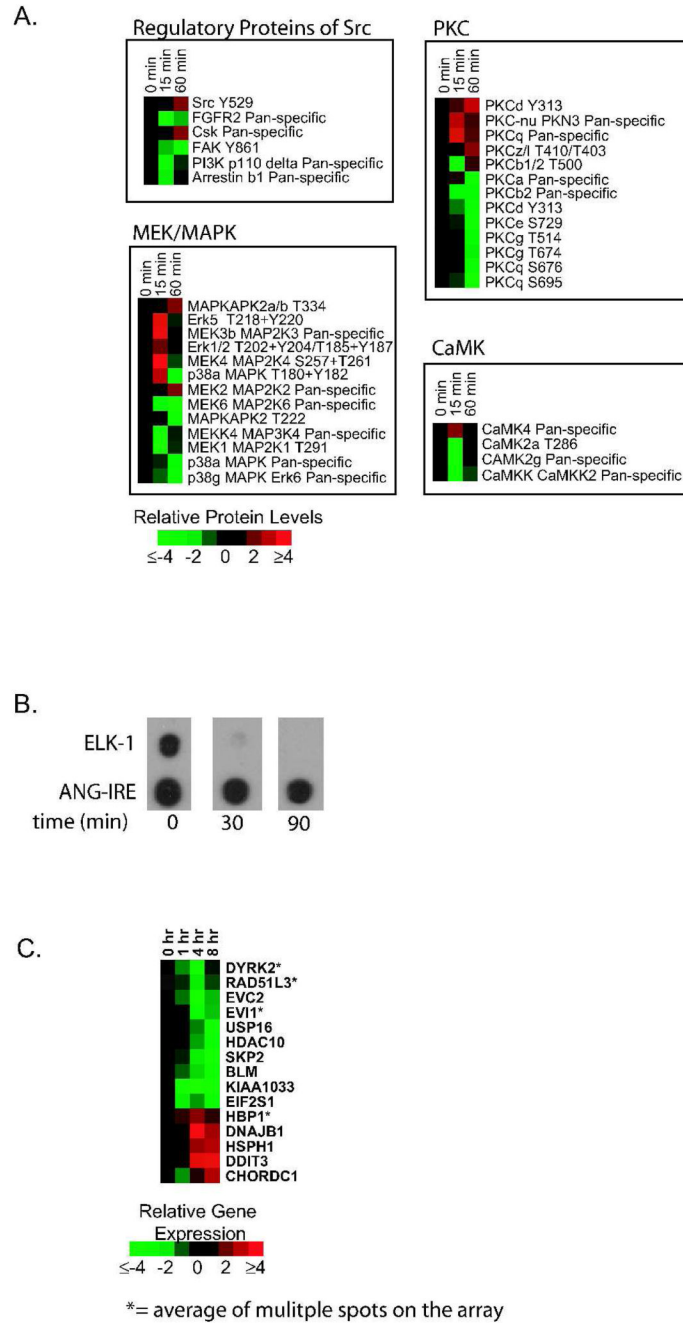
Figure 4.
Parthenolide attenuates src signaling. (A) Protein microarray of prostate cancer cells (DU145) treated with PTL (15 or 60 min). Relative protein level changes are indicated by the color bar. Red indicates an increase, green indicates a decrease and black indicates no change. Time points (0, 15 and 60 min) are shown at the top of each protein cluster: regulatory proteins of src (top left panel), PKC proteins (top right panel), MEK/MAPK proteins (bottom left) and CaMK proteins (bottom right). (B) Regulation of ELK-1 binding in DU145 cells treated with PTL at 0, 30 and 90 min. Transcriptional binding was determined using Panomic's DNA/ protein combo array. Loss of ELK-1 binding is shown on the top panel. Bottom panel is ANG-IRE, an adjacent spot with small differences in binding activity to demonstrate specificity and

equal hybridization. (C) ELK-1-dependent gene expression changes of DU145 cells treated with PTL (1, 4, or 8 hr). Relative gene expression changes are indicated by the color bar. Red represents an increase, green represents a decrease and black represents no change. * denotes an average of multiple spots on the array.
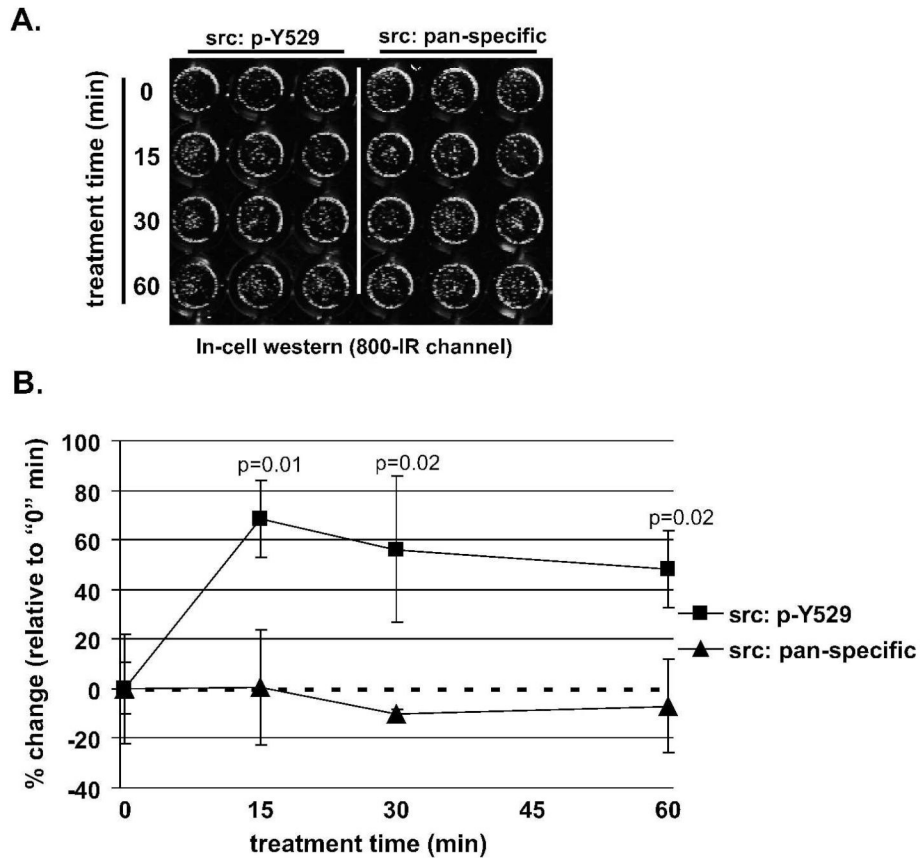
Figure 5.
PTL increases src phosphorylation at tyrosine 529 in CD44^{hi} tumor-initiating DU145 cells. (A) Representative image of an In-cell western assay for src activity. PTL treatment times (0, 15, 30 and 90 min) are indicated on the left side. The left panel indicates phosphorylation of src at tyrosine 529 (p-Y529), a measure of its activity and the right panel shows total src expression (pan-specific). Note that the green color was artificially generated to illustrate immunostaining image acquired from the infrared (IR) dye. (B) Quantitation of the In-cell western assay for src activity. Percent changes were calculated as fold changes relative to untreated control (0 time point) and presented as mean $\pm$ SD. The signal intensities for p-Y529 and pan-specific src were normalized to TO-PRO-3 iodide fluorescence (not shown). P-values (n=3) compare percent changes of p-Y529 with percent changes of pan-specific src.
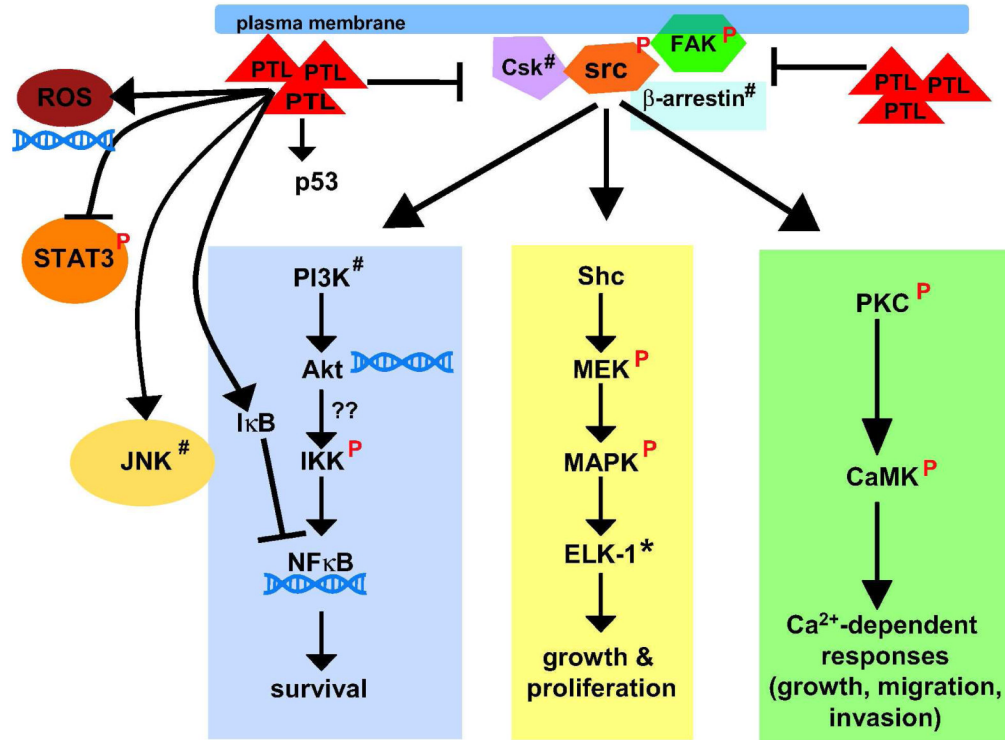
Figure 6.
Molecular mechanism of parthenolide induced death of prostate cancer cells. PTL-induced cell death affects a number of prostate cancer-related signaling pathways, including: src and src-related signaling components, reactive oxygen species (ROS), NFκB signaling, p53, STAT3 activity and JNK. (*) indicates DNA binding change, (DNA double-helix) indicates gene expression change, (P) phosphorylation change and (#) indicates protein level change.